

# BACKSTEPPING SLIDING MODE CONTROL AND 1<sup>ST</sup> ORDER SLIDING MODE CONTROL FOR WHEEL SLIP TRACKING: A COMPARISON

SO SÁNH ĐIỀU KHIỂN TRƯỢT CUỐN CHIẾU VÀ ĐIỀU KHIỂN TRƯỢT BẬC NHẤT TRONG THEO DÕI ĐỘ TRƯỢT BÁNH XE

Nguyen The Anh<sup>1</sup>, Le Quoc Manh<sup>1</sup>, Pham Xuan Duc<sup>1</sup>,  
Le Duc Thinh<sup>1</sup>, Nguyen Tung Lam<sup>1,\*</sup>

DOI: <https://doi.org/10.57001/huih5804.2023.055>

## ABSTRACT

The wheel slip controller serves as the cornerstone of the anti-lock braking system (ABS). The friction between the road and tire, according to research, is a nonlinear function of wheel slip. Therefore, it is necessary to investigate and test a nonlinear robust wheel slip controller. The nominal model in this study is a quarter-car model. In this research, a backstepping sliding mode controller (BSMC) and a first order sliding mode controller (FOSMC) are the 2 types of controller methods that are suggested and compared. The extended state observer (ESO) is used with the design of the BSMC in order to estimate the total uncertainty. A simulation software is then used to verify the viability of the suggested controllers.

**Keywords:** *Wheel slip control, sliding mode control, backstepping control, extended state observer.*

## TÓM TẮT

Điều khiển độ trượt của bánh xe là nền tảng cho hệ thống chống bó phanh (ABS). Các nghiên cứu đã chỉ ra rằng, hệ số ma sát giữa mặt đường và lốp xe, là một hàm phi tuyến của độ trượt. Do đó, nghiên cứu và thử nghiệm về một bộ điều khiển phi tuyến mạnh mẽ là rất cần thiết. Mô hình được sử dụng trong nghiên cứu này là mô hình một phần tư xe. Bộ điều khiển trượt cuốn chiếu và bộ điều khiển trượt bậc nhất là hai loại bộ điều khiển được đưa ra và so sánh trong bài nghiên cứu này. Bộ quan sát trạng thái mở rộng (ESO) được sử dụng cùng với bộ điều khiển trượt cuốn chiếu để ước lượng tổng thành phần bất định của hệ thống. Một phần mềm mô phỏng được thực hiện để xác minh tính khả thi của những bộ điều khiển được đề xuất.

**Từ khóa:** *Điều khiển độ trượt, điều khiển bước lùi, điều khiển trượt, bộ quan sát trạng thái mở rộng.*

<sup>1</sup>School of Electrical and Electronic Engineering, Hanoi University of Science and Technology

\*Email: lam.nguyentung@hust.edu.vn

Received: 24/10/2022

Revised: 03/02/2023

Accepted: 15/3/2023

## 1. INTRODUCTION

The anti-lock braking system is one of the most essential components in modern vehicles for enhancing

the safety of the driver and passengers (ABS) [1]. To satisfy the demand, numerous onboard ABS have been developed. For instance, the Electronic Stability Controller (ESC), which uses the active braking system to increase lateral stability, has been used [2]; the automatic emergency braking (AEB) system can direct brake torque or desired wheel slip to avoid accidents and reduce casualties at the same time [3]. In particular, the current trend in wheel slip control is a shift from simple wheel locking avoidance to continuous wheel slip tracking control [4].

Recent years have seen a significant amount of research on this topic. The implementations for wheel slip control fall into two categories: a rule-based strategy based on the wheel slip ratio and direct torque control techniques based on the vehicle or wheel model [5]. Challa et al. suggested a combined 3-phase rule-based Slip and Wheel Acceleration Threshold Algorithm for Anti-lock Braking in HCRVs, and gives a method for determining the specific threshold values that make up the rule-based ABS algorithm [6]. Pasillas-Lépine et al. introduced a novel class of anti-lock brake algorithms (that make use of wheel deceleration logic-based switchings) and a straightforward mathematical foundation that describes their operation [7]. Jing et al. introduced a switching control strategy built on the Lyapunov approach in the Filippov framework, which effectively takes into consideration the discontinuous dynamics of hydraulic actuators [8].

The model-based wheel slip control strategy has fewer tuning thresholds than the rule-based approach described in the preceding paragraph and may be able to achieve continuous tracking control for wheel slip. In Solyom et al., a gain-scheduled controller that controls tire-slip is proposed along with a design model, and the proposed controller outperformed several other examined methods in terms of deceleration [9]. A second-order sliding-mode traction force controller for cars has been proposed by Amodeo et al., and simulation results have shown that the proposed control system might be

effective [10]. Mirzaei and Mirzaeinejad constructed the quarter-vehicle model using the Dugoff tire model as the nominal model and proposed an ideal predictive approach to develop a nonlinear robust wheel slip controller [11]. The study of a model-based wheel slip control system combined with gain scheduling is the contribution of Johansen et al.. The model is linearized about the nominal wheel slip and the vehicle speed is considered as a slowly time-varying parameter [12]. However, the impact of external disturbances was not discussed in any of the research studies mentioned above; only the influence of model uncertainty on system performance was examined. Designing a model-based wheel slip controller that includes model uncertainties and external disturbances is needed.

Due to the backstepping method's straightforward and adaptable design process as well as its efficiency in applying control to nonlinear systems, it has been studied [13-15]. The backstepping strategy is vulnerable to aggregated uncertainty, though. To deal with lumped uncertainty, the sliding mode control method is expanded to include the backstepping method.

In our article, Zhang and Li [4] serves as the starting point. Following that article, we offer a similar BSMC with the same dynamic model's parameters. However, we employ the ESO in place of the radial basis function neural network (RBFNN) to estimate the lumped uncertainty. The weakness in Zhang and Li's work is that the proposed controller uses a derivative form of both the torque brake and the wheel slip, even though using a derivative form in a controller is strongly discouraged. Our paper's contribution is two different types of controllers to address the weaknesses mentioned.

In this paper, a BSMC combined with the ESO is introduced to design a wheel slip controller based on a quarter-car model. ESO is used to estimate the state variables and the total uncertainty of the model without the need for the derivative form of the wheel slip. Moreover, we provided another control method for comparison: a simple FOSMC, which also does not need both the derivative form of the torque brake and the wheel slip. Finally, simulations are used to compare the performance of both controllers.

The remaining sections are arranged as follows: In the second part, the dynamic model is considered; in the third part, the controller design is proposed with two small parts: BSMC and FOSMC; in the fourth part, results of simulations using Matlab/Simulink are presented; and the conclusion of the work is presented in the Conclusion.

**2. THE DYNAMIC MODEL**

Figure 1 illustrates the wheel slip controller design using a basic yet efficient quarter-vehicle mode.

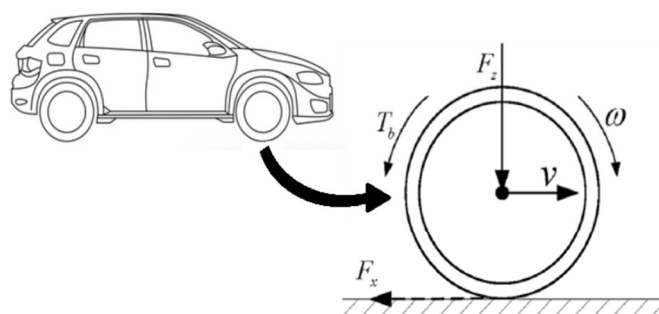


Figure 1. The quarter-vehicle model

The dynamic equations for the quarter-car model is:

$$\begin{cases} J\dot{\omega} = rF_x - T_b \\ m\dot{v} = -F_x \end{cases} \tag{1}$$

where J is the wheel inertia, ω is the angular velocity of the wheel, r is the wheel radius, F<sub>x</sub> is the longitudinal tire-road contact force, T<sub>b</sub> is the brake torque, m is mass of the quarter-car and v is the vehicle's longitudinal speed.

The wheel slip is

$$\lambda = \frac{v - \omega r}{v} \tag{2}$$

The derivation of equation (2) is:

$$\dot{\lambda} = \frac{1}{v} [(1 - \lambda)\dot{v} - \dot{\omega}r] \tag{3}$$

The relationship between the wheel slip and the tire-road friction coefficient is explained by the tire model developed by Burckhardt [16]:

$$\mu(\lambda) = \vartheta_1(1 - e^{-\lambda\vartheta_2}) - \lambda\vartheta_3 \tag{4}$$

where  $\vartheta_1, \vartheta_2, \vartheta_3$  are the coefficients of a specific road's condition.

F<sub>x</sub> can be rewritten as F<sub>x</sub> = F<sub>z</sub>μ(λ), with F<sub>z</sub> is the vertical force at the tire-road contact point.

Through transformation, we can achieve:

$$\dot{x}_2 = f(x_1, x_2) + Gu \tag{5}$$

where  $x_1 = \lambda, x_2 = \dot{x}_1, u = \dot{T}_b,$   
 $f(x_1, x_2) = -(1/v)[-2(F_z\mu(x_1)/m)x_2 + (((1-x_1)/m) + (r^2/J))F_z\dot{\mu}(x_1)],$   
 $G = r/Jv.$

Assume that both model uncertainties and external disturbances are present in the model uncertainty, equation (5) can be expressed as [4]:

$$\begin{aligned} \dot{x}_2 &= (f(x_1, x_2) + \Delta f) + (G + \Delta G)u + d \\ &= f(x_1, x_2) + Gu + D_x \end{aligned} \tag{6}$$

where Δf and ΔG are the model uncertainties, d is the external disturbances and D<sub>x</sub> = Δf + ΔGu + d is the total uncertainty while we assume  $|D_x| \leq L.$

From the dynamic equations of the quarter-car model, we can get the state equation for the model of the wheel slip dynamics, which is used to develop the BSMC [4]:

$$\begin{cases} \dot{x}_1 = x_2 \\ \dot{x}_2 = f(x_1, x_2) + Gu + D_x \end{cases} \quad (7)$$

Substitute  $\dot{\omega}$  and  $\dot{v}$  from equation (1) into equation (3):

$$\begin{aligned} \dot{\lambda} &= \frac{1}{v} \left[ (1-\lambda) \frac{-F_z \mu(\lambda)}{m} - \frac{r F_z \mu(\lambda) - T_b}{J} \right] \\ &= \frac{1}{v} \left[ (\lambda-1) \frac{F_z \mu(\lambda)}{m} - \frac{r^2 F_z \mu(\lambda)}{J} \right] + \frac{r}{Jv} T_b \end{aligned} \quad (8)$$

Select  $x'_1 = \lambda, u = T_b$ , and with the same reasoning about lumped uncertainty, a first order equation for the wheel slip can be obtained, which is used to develop the FOSMC:

$$\dot{x}'_1 = F(x'_1) + Gu + D'_x \quad (9)$$

where  $F(x'_1) = (1/v)[(x'_1 - 1)(F_z \mu(x'_1)/m) - (r^2 F_z \mu(x'_1)/J)]$ ,  $G = r/Jv$  and  $D'_x$  is the lumped uncertainty while we assume  $|D'_x| \leq D$ .

### 3. CONTROLLER DESIGN

#### 3.1. Backstepping Sliding mode controller with ESO

Based on the standard ESO design, from (7), set  $x_3 = D_x$ , then  $\dot{x}_3 = \dot{D}_x$ . The original system can then be turned to:

$$\begin{cases} \dot{x}_1 = x_2 \\ \dot{x}_2 = x_3 + Gu + f(x_1, x_2) \\ \dot{x}_3 = \dot{D}_x \end{cases} \quad (10)$$

The ESO is designed as:

$$\begin{cases} \dot{\hat{x}}_1 = \hat{x}_2 - \frac{k_1}{\epsilon} (\hat{x}_1 - x_1) \\ \dot{\hat{x}}_2 = \hat{x}_3 - \frac{k_2}{\epsilon^2} (\hat{x}_1 - x_1) + Gu + f(\hat{x}_1, \hat{x}_2) \\ \dot{\hat{x}}_3 = -\frac{k_3}{\epsilon^3} (\hat{x}_1 - x_1) \end{cases} \quad (11)$$

The goal of ESO are:

$$\hat{x}_1 \rightarrow x_1, \hat{x}_2 \rightarrow x_2, \hat{x}_3 \rightarrow D_x \text{ as } t \rightarrow \infty$$

where  $\hat{x}_1, \hat{x}_2$  and  $\hat{x}_3$  are states of the ESO,  $\epsilon > 0, k_1, k_2, k_3$  are positive constants, polynomial  $s^3 + k_1 s^2 + k_2 s + k_3$  is Hurwitz.

Define

$$\boldsymbol{\eta} = [\eta_1 \quad \eta_2 \quad \eta_3]^T$$

$$\text{where } \eta_1 = \frac{x - \hat{x}_1}{\epsilon^2}, \eta_2 = \frac{x_2 - \hat{x}_2}{\epsilon}, \eta_3 = D_x - \hat{x}_3.$$

The following equations can be obtained through transformation:

$$\begin{aligned} \epsilon \dot{\eta}_1 &= \frac{\dot{x}_1 - \dot{\hat{x}}_1}{\epsilon} \\ &= \frac{1}{\epsilon} \left[ x_2 - \left[ \hat{x}_2 - \frac{k_1}{\epsilon} (\hat{x}_1 - x_1) \right] \right] \\ &= \frac{-k_1}{\epsilon^2} (x_1 - \hat{x}_1) + \frac{1}{\epsilon} (x_2 - \hat{x}_2) \\ &= -k_1 \eta_1 + \eta_2 \\ \epsilon \dot{\eta}_2 &= \dot{x}_2 - \dot{\hat{x}}_2 \\ &= f(x_1, x_2) + Gu + D_x - \left( \hat{x}_3 - \frac{k_2}{\epsilon^2} (\hat{x}_1 - x_1) + Gu + f(\hat{x}_1, \hat{x}_2) \right) \\ &= -\frac{k_2}{\epsilon^2} (x_1 - \hat{x}_1) + (D_x - \hat{x}_3) + [f(x_1, x_2) - f(\hat{x}_1, \hat{x}_2)] \\ &= -k_2 \eta_1 + \eta_3 + [f(x_1, x_2) - f(\hat{x}_1, \hat{x}_2)] \\ \epsilon \dot{\eta}_3 &= \epsilon (\dot{D}_x - \dot{\hat{x}}_3) \\ &= \epsilon \left[ \dot{D}_x + \frac{k_3}{\epsilon^3} (\hat{x}_1 - x_1) \right] \\ &= -\frac{k_3}{\epsilon^2} (x_1 - \hat{x}_1) + \epsilon \dot{D}_x \\ &= -k_3 \eta_1 + \epsilon \dot{D}_x \end{aligned}$$

The formula of the observation error system is:

$$\epsilon \dot{\boldsymbol{\eta}} = \mathbf{A} \boldsymbol{\eta} + \mathbf{B} \tilde{f} + \epsilon \mathbf{C} \dot{D}_x \quad (12)$$

Where

$$\mathbf{A} = \begin{pmatrix} -k_1 & 1 & 0 \\ -k_2 & 0 & 1 \\ -k_3 & 0 & 0 \end{pmatrix}, \mathbf{B} = \begin{pmatrix} 0 \\ 1 \\ 0 \end{pmatrix}, \mathbf{C} = \begin{pmatrix} 0 \\ 0 \\ 1 \end{pmatrix}, \tilde{f} = f(x_1, x_2) - f(\hat{x}_1, \hat{x}_2)$$

The characteristic equation of  $\mathbf{A}$  is

$$\begin{aligned} |\lambda \mathbf{I} - \mathbf{A}| &= \begin{vmatrix} \lambda + k_1 & -1 & 0 \\ k_2 & \lambda & -1 \\ k_3 & 0 & \lambda \end{vmatrix} \\ &= 0 \end{aligned}$$

then

$$(\lambda + k_1) \lambda^2 + k_2 \lambda + k_3 = 0$$

and

$$\lambda^3 + k_1 \lambda^2 + k_2 \lambda + k_3 = 0 \quad (13)$$

If  $k_1, k_2, k_3$  is chosen so that  $\mathbf{A}$  is Hurwitz, then for any given symmetric positive definite matrix  $\mathbf{Q}$ , there exists a unique symmetric positive definite matrix  $\mathbf{P}$  satisfying the Lyapunov function as follows:

$$\mathbf{A}^T \mathbf{P} + \mathbf{P} \mathbf{A} + \mathbf{Q} = 0 \quad (14)$$

Define the Lyapunov function as follows:

$$V_0 = \epsilon \boldsymbol{\eta}^T \mathbf{P} \boldsymbol{\eta} \quad (15)$$

The derivation of  $V_0$  is:

$$\begin{aligned} \dot{V}_0 &= \varepsilon \eta^T P \eta + \varepsilon \eta^T P \dot{\eta} \\ &= [A \eta + B \tilde{f} + \varepsilon C \dot{D}_x]^T P \eta + \eta^T P [A \eta + B \tilde{f} + \varepsilon C \dot{D}_x] \\ &= \eta^T A^T P \eta + (B \tilde{f})^T P \eta + \varepsilon (C \dot{D}_x)^T P \eta + \eta^T A P h \\ &\quad + (B \tilde{f}) P \eta^T + \varepsilon (C \dot{D}_x) P \eta^T \\ &= \eta^T (A^T P + P A) \eta + 2 \eta^T P B \tilde{f} + 2 \eta^T P \varepsilon C \dot{D}_x \\ &\leq -\eta^T Q \eta + 2 \|\eta\| \cdot \|\mathbf{P} B\| \cdot |\tilde{f}| + 2 \varepsilon \|\eta\| \cdot \|\mathbf{P} C\| \cdot |\dot{D}_x| \end{aligned}$$

and

$$\dot{V}_0 \leq -\lambda_{\min}(\mathbf{Q}) \|\eta\|^2 + 2 \|\eta\| \|\mathbf{P} B\| |\tilde{f}| + 2 \varepsilon L \|\mathbf{P} C\| \|\eta\|$$

in which  $-\lambda_{\min}(\mathbf{Q})$  is the minimum eigenvalue of  $\mathbf{Q}$ . To get  $\dot{V}_0 \leq 0$ , the coefficient  $\varepsilon$  is designed to satisfy the following condition:

$$\lambda_{\min}(\mathbf{Q}) \|\eta\|^2 - 2 \|\eta\| \|\mathbf{P} B\| |\tilde{f}| - 2 \varepsilon L \|\mathbf{P} C\| \|\eta\| > 0$$

then the observer error  $\eta$  is asymptotic convergence.

Design  $\varepsilon$  as

$$\frac{1}{\varepsilon} = R = \sigma \frac{1 - e^{-\lambda_1 t}}{1 + e^{-\lambda_2 t}}, 0 \leq t \leq t_{\max} \quad (16)$$

where  $\sigma, \lambda_1, \lambda_2$  are positive constants. Then

$$\lim_{\varepsilon \rightarrow 0} \bar{x}_1 = x_1, \lim_{\varepsilon \rightarrow 0} \bar{x}_2 = x_2, \lim_{\varepsilon \rightarrow 0} \bar{x}_3 = D_x$$

Define  $e_1$  such that

$$e_1 = x_1 - x_d \quad (17)$$

where  $x_d$  is the desired wheel slip. Therefore, we have:

$$\dot{e}_1 = \dot{x}_1 - \dot{x}_d = x_2 - \dot{x}_d$$

Select the Lyapunov candidate function as

$$V_1 = \frac{1}{2} e_1^2 \quad (18)$$

Therefore,

$$\dot{V}_1 = e_1 \dot{e}_1 = e_1 (x_2 - \dot{x}_d)$$

In order to realize  $\dot{V}_1 < 0$ , choose sliding variable

$$s = c_1 e_1 + \dot{e}_1 = x_2 + c_1 e_1 - \dot{x}_d \quad (19)$$

( $c_1 > 0$ ). Then  $x_2 = s - c_1 e_1 + \dot{x}_d$ . Therefore,

$$\dot{V}_1 = e_1 s - c_1 e_1^2$$

If  $s = 0$  then  $\dot{V}_1 < 0$ . Define another Lyapunov candidate function

$$V_2 = V_1 + \frac{1}{2} s^2 \quad (20)$$

The derivative of  $s$  is:

$$\dot{s} = \dot{x}_2 + c_1 \dot{e}_1 - \ddot{x}_d = f(x_1, x_2) + Gu + D_x + c_1 \dot{e}_1 - \ddot{x}_d, \text{ then}$$

$$\begin{aligned} \dot{V}_2 &= \dot{V}_1 + s \dot{s} \\ &= e_1 s - c_1 e_1^2 + s(f(x_1, x_2) + Gu + D_x + c_1 \dot{e}_1 - \ddot{x}_d) \end{aligned}$$

Let the observing sliding mode variable be  $\hat{s} = \hat{e}_2 + c \hat{e}_1$ , where  $\hat{e}_1 = \bar{x}_1 - x_d$  and  $\hat{e}_2 = \bar{x}_2 - \dot{x}_d$ .

To get  $\dot{V}_2 < 0$ , choose control signal  $u$  that

$$u = \frac{1}{G} (-f(x_1, x_2) - c_2 \hat{s} - \hat{e}_1 - c_1 \dot{\hat{e}}_1 + \ddot{x}_d - \eta \operatorname{sgn}(\hat{s}) - \bar{x}_3) \quad (21)$$

Where  $c_2 > 0, \eta > 0$ . Therefore,

$$\dot{V}_2 = s(e_1 - \hat{e}_1) + s(D_x - \ddot{x}_3) + c_1(\dot{e}_1 - \dot{\hat{e}}_1) - c_1 e_1^2 - c_2 s \hat{s} - \eta s \operatorname{sgn}(\hat{s}) < 0$$

As a result, when  $t \rightarrow \infty, e_1 \rightarrow 0$  and  $e_2 \rightarrow 0$ .

### 3.2. First-order sliding mode controller

Based on the standard sliding mode control method, we choose  $e_1$  such that:

$$e_1 = x_d - x'_1 \quad (22)$$

where  $x_d$  is the desired wheel slip. Therefore, we have:

$$\dot{e}_1 = \dot{x}_d - \dot{x}'_1 \quad (23)$$

Define the sliding mode surface  $s = ce$ , where  $c$  is a positive constant. Note that:

$$\dot{s} = c \dot{e} = c(\dot{x}_d - \dot{x}'_1) \quad (24)$$

Select the Lyapunov candidate function as:

$$V_1 = \frac{1}{2} s^2 \quad (25)$$

The derivative of  $V_1$  is given by:

$$\begin{aligned} \dot{V}_1 &= s \dot{s} = s(c \dot{x}_d - c \dot{x}'_1) \\ &= cs(\dot{x}_d - F(x'_1) - Gu - D'_x) \end{aligned} \quad (26)$$

In order to get  $\dot{V}_1 < 0$ , choose the control signal  $u$  such that:

$$u = u_{eq} + u_{sw} \quad (27)$$

$$\text{where } u_{eq} = \frac{1}{G} (-F(x'_1) + \dot{x}_d), u_{sw} = \frac{1}{G} K \operatorname{sgn}(s)$$

To satisfy the reaching conditions of sliding mode control  $s \dot{s} \leq -\eta |s|, \eta > 0, K$  is chosen as  $K = D + \eta$ .

Therefore, we can get:

$$\dot{V}_1 = -cKs \operatorname{sgn}(s) - csD'_x \leq -c\eta |s| < 0 \quad (28)$$

### 4. SIMULATION RESULTS

The designed controllers are simulated using MATLAB/Simulink. We test the designed controllers on a flat, dry asphalt road using step function as the desired wheel slip. The quarter-car model's parameters are  $m = 354\text{kg}, J = 0.9\text{kgm}^2$ , and  $r = 0,310\text{m}$ .  $F_z = 3540\text{N}$  is the vertical force at the point where the tire and road come into contact. The car's initial speed is  $v = 27.78\text{m/s}$ , and the simulation ends when it slows to  $3\text{m/s}$ . Assuming the disturbance is a torque represented as a sine function, added to the angular speed dynamic equations at a frequency of  $2\pi\text{rad/s}$  and an attitude of  $750\text{Nm}$ .

The parameters of the designed ESO are chosen as follows in order to achieve precise tracking of the uncertainty:  $\sigma = 5000, \lambda_1 = \lambda_2 = 3, k_1 = 6, k_2 = 11, k_3 = 6$ . The

designed BSMC parameters are chosen as:  $c_1 = 300$ ,  $c_2 = 200$  and  $\eta = 10$ .

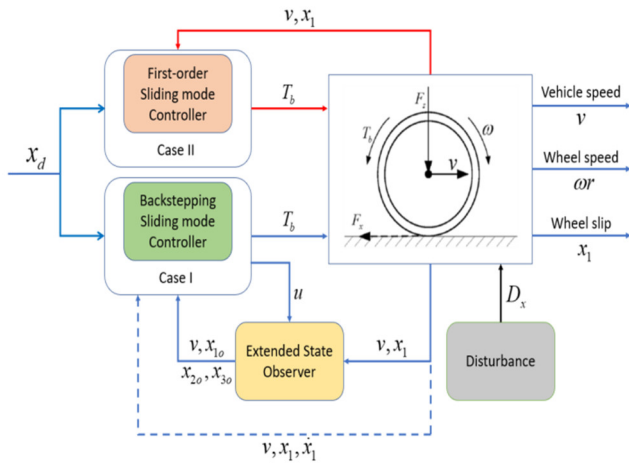


Figure 2. Block diagram of BSMC with ESO and FOSMC. In case I, the BSMC are tested with and without ESO. In case II, FOSMC is simulated

To achieve precise wheel slip tracking, the following parameters of the FOSMC are selected:  $c = 200$  and  $K = 100$ . In order to reduce chattering in the simulation, we can replace  $\text{sgn}(s)$  by  $\tanh(s)$ .

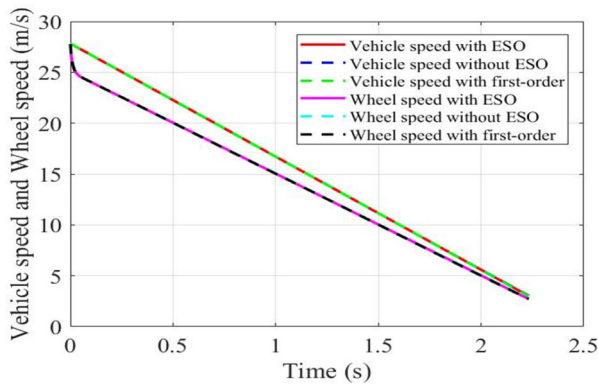


Figure 3. Vehicle speed and wheel speed

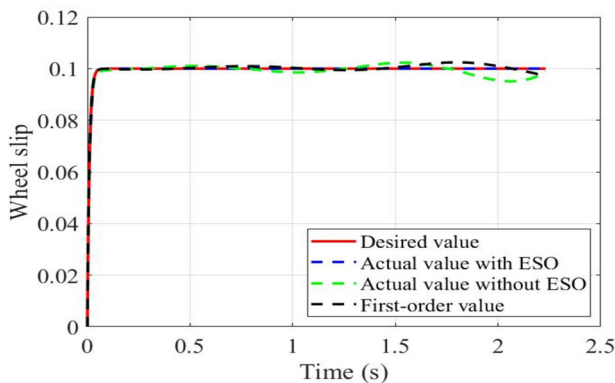


Figure 4. Wheel slip

The step function's final value is set to 0.1. Figure 3 shows that the wheel speed and the vehicle speed successfully slowed down in a reasonable amount of time in both controllers. The result showed that the wheel speed

with both controllers can successfully reduce the impact of the uncertainty and provide more stable vehicle speed and wheel speed decreasing. Comparisons between the desired wheel slip, the actual wheel slip with and without ESO, the FOSMC value are shown in Figure 4. The actual value with ESO is the closest and most stable to the desired wheel slip, followed by the FOSMC value. The actual value without ESO is the least stable and is highly vulnerable to uncertainty. Figure 5 shows the torque brake generated in both controllers. Figure 6 demonstrates how well the ESO is able to estimate the overall system uncertainty.

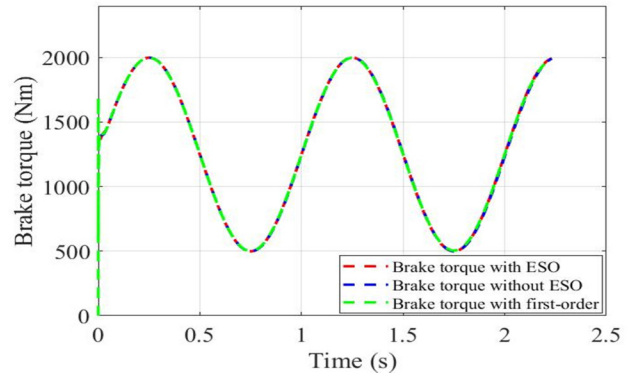


Figure 5. Brake torque

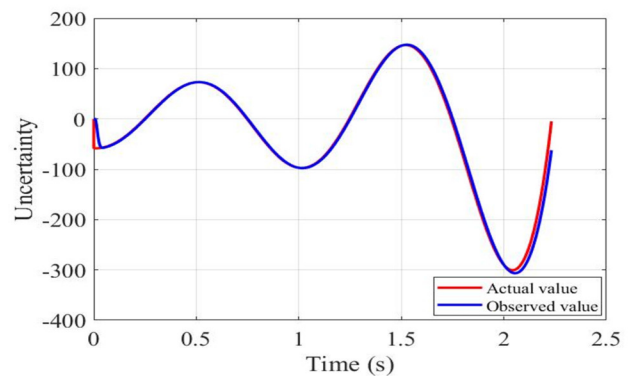


Figure 6. Uncertainty and estimated value

### 5. CONCLUSION

This study presents a comparison between the backstepping sliding mode control strategy and the first order sliding mode control strategy for the design of a wheel slip controller, where the model is a quarter-vehicle model with uncertainty. The total model uncertainty can be precisely tracked by the extended state observer using designed parameters. Finally, the effectiveness of the suggested controllers is tested, using simulations on a flat, dry asphalt road with step function as the desired wheel slip.

In future work, the slip ratio observer needs to be taken into account because it is impossible to precisely measure the vehicle speed. Additionally, since the longitudinal force and vertical force at the point of contact between the tire and the road have an unidentified scaling factor, an adaptive control technique must be combined with the suggested controllers.

## REFERENCES

- [1]. A. Harifi, A. Aghagolzadeh, G. Alizadeh, M. Sadeghi, 2008. *Designing a sliding mode controller for slip control of antilock brake systems*. Transp. Res. part C Emerg. Technol., vol. 16, no. 6, pp. 731–741.
- [2]. I. Youn, E. Youn, M. A. Khan, L. Wu, M. Tomizuka, 2015. *Combined effect of electronic stability control and active tilting control based on full-car nonlinear model*. in Proceedings of the Dynamics of Vehicles on Roads and Tracks: Proceedings of the 24th Symposium of the International Association for Vehicle System Dynamics, Graz, Austria, pp. 17–21.
- [3]. M. Segata, R. Lo Cigno, 2013. *Automatic emergency braking: Realistic analysis of car dynamics and network performance*. IEEE Trans. Veh. Technol., vol. 62, no. 9, pp. 4150–4161.
- [4]. J. Zhang, J. Li, 2018. *Adaptive backstepping sliding mode control for wheel slip tracking of vehicle with uncertainty observer*. Meas. Control, vol. 51, no. 9–10, pp. 396–405.
- [5]. D. Yin, N. Sun, D. Shan, J. S. Hu, 2017. *A multiple data fusion approach to wheel slip control for decentralized electric vehicles*. Energies, vol. 10, no. 4, p. 461.
- [6]. A. Challa, K. Ramakrishnan, P. V. Gaurkar, S. C. Subramanian, G. Vivekanandan, S. Sivaram, 2022. *A 3-phase combined wheel slip and acceleration threshold algorithm for anti-lock braking in heavy commercial road vehicles*. Veh. Syst. Dyn., vol. 60, no. 7, pp. 2312–2333.
- [7]. I. Ait-Hammouda, W. Pasillas-Lépine, 2008. *Jumps and synchronization in anti-lock brake algorithms*. in AVEC 2008.
- [8]. H. Jing, Z. Liu, H. Chen, 2011. *A switched control strategy for antilock braking system with on/off valves*. IEEE Trans. Veh. Technol., vol. 60, no. 4, pp. 1470–1484.
- [9]. S. Solyom, A. Rantzer, J. Lüdemann, 2004. *Synthesis of a model-based tire slip controller*. Veh. Syst. Dyn., vol. 41, no. 6, pp. 475–499.
- [10]. M. Amodeo, A. Ferrara, R. Terzaghi, C. Vecchio, 2009. *Wheel slip control via second-order sliding-mode generation*. IEEE Trans. Intell. Transp. Syst., vol. 11, no. 1, pp. 122–131.
- [11]. M. Mirzaei, H. Mirzaeinejad, 2012. *Optimal design of a non-linear controller for anti-lock braking system*. Transp. Res. part C Emerg. Technol., vol. 24, pp. 19–35.
- [12]. T. A. Johansen, I. Petersen, J. Kalkkuhl, J. Ludemann, 2003. *Gain-scheduled wheel slip control in automotive brake systems*. IEEE Trans. Control Syst. Technol., vol. 11, no. 6, pp. 799–811.
- [13]. F. Mazenc, P. A. Bliman, 2006. *Backstepping design for time-delay nonlinear systems*. IEEE Trans. Automat. Contr., vol. 51, no. 1, pp. 149–154.
- [14]. A. Das, F. Lewis, K. Subbarao, 2009. *Backstepping approach for controlling a quadrotor using lagrange form dynamics*. J. Intell. Robot. Syst., vol. 56, no. 1, pp. 127–151.
- [15]. Z.J. Wu, X.J. Xie, P. Shi, Y. Xia, 2009. *Backstepping controller design for a class of stochastic nonlinear systems with Markovian switching*. Automatica, vol. 45, no. 4, pp. 997–1004.
- [16]. M. Burckhardt, 1993. *Fahrwerktechnik: Radschlupf-Regelsysteme*. Vogel-Verlag, Wurtzbg., vol. 36.

## THÔNG TIN TÁC GIẢ

Nguyễn Thế Anh, Lê Quốc Mạnh, Phạm Xuân Đức, Lê Đức Thịnh,  
Nguyễn Tùng Lâm

Trường Điện - Điện tử, Đại học Bách khoa Hà Nội